BMC Oral Health

RESEARCH

Open Access

Evaluation of mechanical properties and color stability of 3D-printed denture base materials following two surface treatments

Eymen Izzettinoglu[1*] and Erdal Eroglu[1]

Abstract

Background Comprehending the synergistic of surface treatments and oral environmental factors is paramount for optimizing the performance of 3D-printed dentures. This study evaluates flexural strength, hardness, roughness, and color stability of 3D-printed resins after two surface treatments and coffee thermocycling, to establish alternative polishing efficacy.

Materials and methods Rectangular test specimens ($64 \times 10 \times 3.3 \pm 0.2$ mm) were fabricated from a conventional heat-cured denture base material (Probase HC, $n = 20$) and four 3D-printed denture base materials (Nextdent; ND, Formlabs; FL, Senertek; ST, Powerresin; PR, $n = 40$ per group), resulting in a total sample size of $N = 180$. Specimens were randomly assigned to undergo either mechanical polishing or glazing, followed by 5000 cycles of coffee thermocycling (CTC). Color change (ΔE_{00}) and surface roughness (Ra) were assessed both prior to and subsequent to CTC. Subsequently, the specimens were subjected to a 3-point bending test and a Vickers microhardness (VH) test. Statistical analysis of the data was performed using descriptive and analytical methods, with a significance level set at $\alpha = 0.05$.

Results The application of Vita Akzent® LC (VA) as a glaze material, while conferring supplementary protection against surface degradation during coffee thermocycling (CTC), resulted in a statistically significant increase in the initial surface roughness (Ra) values across all experimental 3D-printed groups ($p < 0.05$). It reduced the ΔE value of the FL group ($p = 0.036$) but did not have a statistically significant impact on the ΔE_{00} of other 3D-printed groups ($p > 0.05$). Additionally, VA enhanced the VH of most 3D-printed groups ($p < 0.05$). It improved the flexural strength of the PR and ST groups but decreased it for the FL group and had no significant effect on the ND group ($p = 0.088$). The mechanically polished specimens demonstrated acceptable Ra, ΔE_{00}, and flexural strength values. However, they showed a lower VH than the glazed specimens.

Conclusion Glaze application resulted in improved mechanical strength and hardness for the majority of 3D-printed groups; however, its capacity to effectively reduce surface roughness and discoloration was consistently limited. Conversely, mechanical polishing maintained its beneficial effects, demonstrating clinically acceptable values across all assessed parameters. Therefore, comprehensive additional investigations are necessitated to fully elucidate the performance characteristics of glaze materials and their interactions with 3D-printed denture base materials.

*Correspondence:
Eymen Izzettinoglu
eymenizzettin.tr@gmail.com

Full list of author information is available at the end of the article

Keywords Additive manufacturing, Denture base, Glaze, Color stability, Mechanical properties

Introduction

Rehabilitation with complete dentures (CDs) remains a viable treatment option for edentulous patients facing limitations such as systemic health, compromised oral health, or financial constraints [1, 2]. Meanwhile, computer-aided design and computer-aided manufacturing (CAD-CAM) technologies have revolutionized CDs fabrication, enabling PMMA-based dentures to be produced through streamlined digital workflows. Compared to traditional methods, the CAD-CAM approach offers several advantages, including simplified laboratory procedures and reduced patient visits. Moreover, in the event of a fracture or loss of a denture, a new prosthesis identical to the original can be easily fabricated using previously stored clinical data [2–5].

Two primary CAM techniques are employed in denture fabrication: subtractive manufacturing (SM) and additive manufacturing (AM). Studies have reported that SM may result in improved mechanical properties and reduced polymerization shrinkage compared to other methods. However, AM offers potential advantages in terms of cost-effectiveness, reduced material waste (less environmental pollution), and efficient production of complex geometries. In addition to these advantages, several studies have demonstrated the clinical suitability of AM-generated dental prostheses [6–10].

Vat polymerization, a core technology within additive manufacturing, has been widely used to produce various dental devices. This process involves solidifying liquid resin to create a three-dimensional object. 3D photopolymerization relies on the principle of polymerizing the liquid resin upon exposure to a specific wavelength of light [11]. Vat polymerization technologies can be categorized based on the light source employed: stereolithography (SLA), direct light processing (DLP), and liquid crystal display-based (LCD) printing, also known as daylight polymer printing (DPP) [11, 12]. In SLA, a building platform is immersed in a liquid polymer resin, which is then polymerized layer-by-layer using ultraviolet (UV) light. In this process, a laser traces the object's cross-section on the resin surface, inducing polymerization. DLP printers utilize a projector or a digital micromirror device (DMD) to project a light mask onto the entire resin layer, enabling simultaneous polymerization [13]. DPP technology employs light from LCD screens to polymerize the photosensitive resin [11].

While 3D-printed dentures hold significant promise, comprehensive investigations into their mechanical, physical, and aesthetic properties are essential to establish their re-liability as an alternative to conventional PMMA dentures [14]. To date, mechanical polishing has been the primary focus of research on improving the surface properties of 3D-printed denture base materials [2, 15, 16]. The utilization of surface sealants as a glazing agent offers a promising approach to minimizing surface roughness (Ra) in resin-based materials by filling the micropores on the prosthesis surface [17–20]. Despite the growing interest in 3D-printed denture base materials, there is a significant dearth of studies investigating the potential benefits of applying glazes and coatings to enhance the properties and performance of these devices [20–23]. Thus, this study aims to investigate the flexural strength, hardness, surface roughness, and color stability of denture base resins produced with different methods and subjected to coffee thermal cycling following two different sur-face treatments.

The null hypothesis stated that there were no significant differences in flexural strength, microhardness, surface roughness, and color stability among conventional heat-polymerized PMMA and 3D-printed denture base resins with two distinct surface treatments after coffee thermocycling.

Materials and methods

This in vitro study used four commercially available, certified denture base resins compatible with different vat polymerization technologies and a conventional heat-cured resin as a control group.

By assuming %80 power and 0.05 level of significance, 20 specimens per group for each test were determined necessary to detect a large effect size of 0.40, as recommended by Cohen [24]. The number of test specimens ($N = 180$) was calculated using a software program (G*Power 3.1.9.2, Heinrich-Heine University, Dusseldorf, Germany).

Specimens' preparation

The specimens ($N = 180$) required for this present study were designed virtually according to ISO 20795-1: 2013 standards ($64 \times 10 \times 3.3 \pm 0.2$ mm) [25] using CAD software (Tinker CAD, Autodesk Inc., USA). The data were then transformed into a standard tessellation language (STL) file to be exported to 3D printers according to the printing system.

3D-printed specimens were fabricated strictly adhering to the manufacturer's guidelines. Table 1 provides a comprehensive overview of the materials employed, their chemical compositions, the brand and model of the 3D printers utilized in this study, and the precise printing parameters of the liquid resin for the specified printer.

Following the 3D printing process, all specimens underwent a standardized post-processing protocol,

Table 1 Presents a comprehensive overview of the 3D printed materials, their compositions, the printers, and the specific printing parameters utilized in this study

Brand name	NextDent Denture 3D+	Denture base resin, FormLabs	Powerresins denture base	Senertek denture base v2
Code	ND	FL	PR	ST
Manufacturer	NextDent B.V., Soesterberg, Netherlands	Formlabs, Somerville, MA, USA	NovaFab Technology Company, Istanbul, Turkey	Senertek group, Izmir, Turkey
Lot Number	WU232N03	BF23F26O	MD1220241015001	SNR202300024
Composition	Ethoxylated bisphenol A dimethacrylate % ≥75 7,7,9(or 7,9,9)-trimethyl-4,13-dioxo-3,14-dioxa-5,12- diazahexadecane-1,16-diyl bismethacrylate % 10–20 2-hydroxyethyl methacrylate % 5–10 Silicon dioxide % 5–10 diphenyl (2,4,6- trimethylbenzoyl) phosphine oxide %1–5 Titanium dioxide < 0,1	Bisphenol A dimethacrylate % 40–60 Urethane dimethacrylate %30–50 Methacrylate monomer % 5–10 Photoinitiator <%3	Esterification products of 4,4′-iso-propylidenediphenol, ethoxylated and 2-methylprop-2-enoic acid %40–60 7,7,9(or 7,9,9)-trimethyl-4,13-dioxo-3,14-dioxa-5,12-diazahexadecane-1,16-diyl bismethacrylate %10–20 Titanium dioxide 5–10% diphenyl (2,4,6- trimethylbenzoyl) phosphine oxide 1–5%	Urethane dimethacrylate %50–75 Trimethylbenzoyl diphenyl phosphine oxide % 0.1-1 The remaining ingredients are undisclosed
Printer	NextDent 5100 3D (NextDent BV, 3D Systems, The Netherlands)	From 3+ (Formlabs, Somerville, MA, USA)	Dentafab Sega (NovaFab Technology Company, Istanbul, Turkey)	3D printer (Sonic Mini 8 K, Phrozen, Hsinchu, Taiwan)
Slicing software	3D Sprint V2 software, 3D Systems	PreForm 3D slicing and printing software (Formlab)	DENTAFAB SOFTWARE 4.0.1	Chitubox V1.9.4 software
Printing technology	Digital light processing (DLP)	Stereolithography (SLA)	Digital light processing (Fast DLP)	Liquid Crystal Display (LCD)
Printing layer thickness	50 µm			
Printing orientations	60 °	40 °	60 °	20 °

encompassing washing and post-curing procedures, in strict adherence to the respective manufacturer's guidelines. Specifically, the NextDent (ND) group was subjected to a dual-chamber washing process utilizing 99.9% ethanol in a Twin Tornado device (Medifive, Incheon, Korea) for a total duration of less than five minutes, comprising a two-minute pre-cleaning phase in ethanol followed by an additional two minutes in fresh ethanol within the second chamber. The FormLabs (FL) group was washed in a Form Wash (Formlabs, Somerville, MA, USA) using 99.9% isopropyl alcohol (IPA) for ten minutes. For the Powerresin (PR) group, resin residues were manually removed using a soft brush dampened with 96% ethanol until all resin remnants were completely eliminated, as recommended by the manufacturer, in lieu of a dedicated washing device. The Senertek (ST) group specimens were washed in a Wash & Cure Machine 2.0 (Anycubic, Shenzhen, China) using 99.9% IPA for five minutes. Subsequent to washing, all specimens were air-dried and allowed to rest for a minimum of ten minutes to ensure complete evaporation of residual alcohol prior to further processing.

For post-curing, the ND group was polymerized in an LC-D Print Box (3D Systems, Vertex Dental B.V., Soesterberg, Netherlands) under an air atmosphere at 60 °C for 30 min, excluding a 15-minute preheating period. The FL group was post-cured in a Form Cure device (Formlabs, Somerville, MA, USA) utilizing a vegetable glycerin environment at 80 °C for 30 min, with each surface cured separately for 30 min. The PR group underwent post-curing in an Otoflash G171 device (NK optics, Baierbrunn, Germany) under a nitrogen atmosphere, with each surface receiving 2500 flashes. The ST group was post-cured in a NOVA3D Fastcure Curing Machine (Shenzhen Nova Robot Technology Co., Ltd, China) using a vegetable glycerin environment for 20 min.

The pressure molding technique fabricated conventional heat-cured (HC) specimens. A stainless metal mold was used to create a wax pattern, which was invested in a flask with Type III gypsum (ReorX®; Alfasan, Eskisehir, Turkey). After the gypsum ad set, the wax was boiled out, and the powder and liquid of the heat-polymerizing acrylic resin (Probase Hot, Ivoclar Vivadent AG, Liechtenstein; Polymer Lot number: YB60YF, Monomer Lot number: Z05SGJ) were mixed according to the manufacturer's recommended ratio (22,5 g:10 ml) using an analytical balance; the mixture was then packed in the mold. The flask was sealed and immersed in cold water. According to the manufacturer's protocol, the water was heated to 100 °C (212 °F) and maintained at a rolling

boil for 45 min. HC bar-shaped specimen surfaces were finished with 600- to 1200-grit silicon carbide abrasive papers (Atlas Waterproof Sheet, Saint-Gobain Abrasives, Turkey) for 10 s [15] and conventionally polished with pumice (BLAUpum, Efes dental, Bursa, Turkey) and polishing paste (Universal Polishing Paste, Ivoclar Vivadent AG, Schaan, Liechtenstein, LOT: Z03T49) until a glossy surface was achieved [15, 23].

Vita Akzent® LC GLAZE was not applied to the HC group. To eliminate residual support markings and achieve a homogeneous surface suitable for subsequent sandblasting, all specimens, including both mechanically polished and glazed groups, underwent silicon carbide application (600-to 1200-grit), as illustrated (Fig. 1). Half of the bar-shaped 3D specimens were sandblasted with 50 µm Al_2O_3 particles at 2 bar pressure. Post-sandblasting, specimens were thoroughly cleaned with oil-free air. A thin layer of VA (Vita Akzent® LC GLAZE, VITA Zahnfabrik, Germany, LOT:97120) was applied to the sandblasted surfaces using a soft brush in a single direction [17, 20].

After a 20-second application time [20], the specimens were light-polymerized for 3 min using a light-polymerization unit (Solidilite V, SHOFU Dental Corp, Japan).

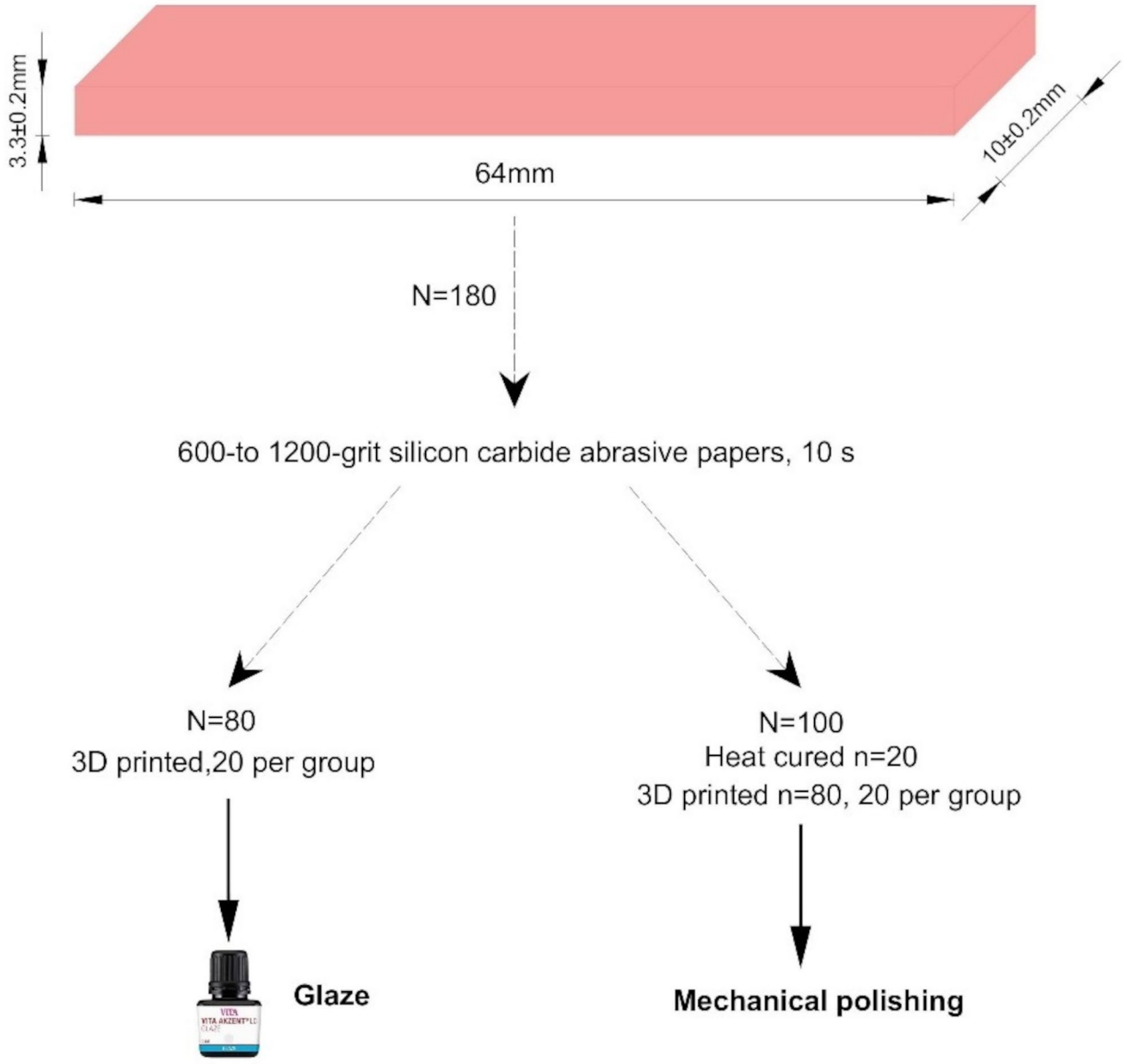

Fig. 1 The flowchart illustrates the distribution of sample sizes across different surface treatment groups

Finally, the glazed surfaces were polished with a polishing paste (Renfert Polish hybrid materials; Renfert GmbH Co., Hilzingen, Germany, LOT:5103000) and a soft goat hairbrush (DENTindex, Turkey), followed by a dry cotton buff to achieve the desired gloss, as per the VitaAkzent® LC GLAZE user guidelines. The remaining half were finished and polished, as for the HC PMMA specimens. (Fig. 1)

The specimens' dimensions were checked using an IP54 Protected digital caliper (Dasqua®, Italy) with 0.01 mm accuracy. They were stored in 37 °C distilled water for 50 ± 2 h in an oven (Binder GmbHED115, Tuttlingen, Germany) to simulate the plasticizing effect of the aqueous intraoral environment on the denture base and to eliminate the unreacted residual monomer [8].

All specimens were cleaned in distilled water in an ultrasonic bath (VGT-1740QTD, Guangzhou Sunlight Medical Equipment Co. Ltd., Guangdong, China) for 10 min [15]. The bar specimens underwent coffee thermocycling (DTS B1, Dentester, Salubris Technica, Istanbul, Turkey) for 5000 cycles (5–55 °C water bath, 30-second dwell time, 10-second transfer time) [15, 16]. The coffee solution was prepared by adding one tablespoon of coffee (Nescafe Classic; Nestle SA) to 177 mL of water, and the solution was refreshed every 12 h [15–17]. After coffee thermocycling, the specimens were brushed 10 times circumferentially with toothpaste and Federal Drug Administration (FDA) certified toothbrushes (GLİMO, HALTRON company, İstanbul, Turkey) under running water. They were then dried to minimize surface stains [15, 16, 26]. The specimens were cleaned again in distilled water in an ultrasonic bath for 10 min and dried with absorbent paper before the roughness testing surface.

Surface roughness measurement

Surface roughness (Ra) was measured at three different locations on each polished and glazed specimen, both prior to and following coffee thermocycling. These measurements were conducted at the center of each specimen, with each point separated by a minimum distance of 0.5 mm. A digital contact profilometer (Surftest SJ-210, Mitutoyo, Tokyo, Japan), with an accuracy of 0.001 µm, was utilized for these measurements. The average of the three readings was subsequently calculated and recorded, in accordance with the methodology outlined by [20].

Before each sample measurement, the profilometer was calibrated using its reference block with a Ra value of 2.970 µm. Surface roughness measurements were conducted using a diamond stylus with a tip radius of 2 µm, a tip angle of 60°, and an ISO 4287:1997 profile. The cut-off value was set to 0.8 mm, the measurement length was 5.6 mm, and the stylus tracking speed was maintained at a constant rate of 0.5 mm/s.

Color stability test

The color was assessed once before and once after coffee thermocycling using a spectrophotometer (Gretag Macbeth ColorEye 7000 A Spectrophotometer; X-Rite, Grand Rapids, MI, USA), which uses the CIE standard (10-degree) human observer characteristics and CIE D65 illuminant in its color estimations [27–29]. The L*, a*, b*, C*, and h° parameters were measured to assess the possible ΔE changes. Colorimetric measurements were conducted at the central point of each specimen against a standardized white background (Foam board, Alex Schoeller ®), with each measurement performed in triplicate [15]. As outlined in the manufacturer's protocol, calibration was achieved using white and black ceramic tiles. The mean of the spectra was then calculated. The CIEDE2000 (ΔE_{00}) formula was used to calculate color change:

$$\Delta E_{00} = \sqrt{\left(\frac{\Delta L'}{K_L S_L}\right)^2 + \left(\frac{\Delta C'}{K_C S_C}\right)^2 + \left(\frac{\Delta H'}{K_H S_H}\right)^2 + R_T \left(\frac{\Delta C'}{K_C S_C}\right)\left(\frac{\Delta H'}{K_H S_H}\right)}$$

where ΔL′, ΔC′, and ΔH′ are the mathematical differences in CIE Lab lightness, chroma, and hue, respectively. S_L,S_C,and S_H are weighting functions. K_L,K_c, and K_H are the terms for the experimental conditions, and those parametric values were set to 1 for this study [2].

To better simulate the clinical performance, the ΔE_{00} values were converted to the National Bureau of Standards (NBS) units by using the following formula: NBS unit = $\Delta E_{00} \times 0.92$ [14, 15].

Before each measurement, the spectrophotometer was calibrated according to the manufacturer's recommendation. The same clinician (E.I.) performed all color measurements under daylight in a temperature and humidity-controlled room.

Microhardness test

Before the Flexural strength test, the surface hardness of the specimens was measured by a microhardness tester (Matsuzawa HWMMT-X3, TTS Unlimited Inc., Osaka, Japan) with a Vickers diamond indenter under a 0.49-N load for 10 s [15]. The diameters of the rectangular indentations were measured under the microscope of the microhardness tester. Three measurements were made for each specimen in different points. The same specimens, having undergone Coffee Thermal Cycling (CTC) treatment, were utilized for both Vickers hardness and 3-point bending tests. To mitigate the potential influence of defects induced by the Vickers hardness indentation on the subsequent flexural strength assessment, Vickers hardness measurements were strategically performed

outside the 50 mm span between the supporting rods used in the 3-point bending test setup. The mean of the three measurements was calculated as the Vickers hardness number.

The three-point bend test

The flexural strength was measured using the three-point bend test and a universal testing machine (Shimadzu AGS-X 10kN; Kyoto, Japan). The load was applied vertically to the center of the specimens at a crosshead speed of 5 mm/min. The load-deflection curves were drawn by a computer connected to the machine. The flexural strength of the specimens was calculated in MPa using the following equation: flexural strength = $3FL/2bd^2$, according to the ISO 20795-1 standard [20, 25], where F is the applied load in N, L is the distance between the center of the supporting rods (50 mm), b is the specimen width (10 mm), and d is the specimen thickness (3.3 mm).

The morphology of the fracture surfaces was examined using a scanning electron microscope (SEM) (SEM-EDS, FEI Quanta Feg 250, Holland) at a magnification of 500x. Specimens exhibiting well-defined, organized, compact, and flat fracture surfaces were classified as brittle fractures, while those displaying irregular, disorganized surfaces were categorized as intermediate fractures [15, 30].

Statistical analysis

Data were analyzed using IBM SPSS Statistics 25 for Windows. Descriptive statistics (mean, standard deviation, minimum, maximum, median) were calculated. Normality was assessed using the Shapiro-Wilk test, and homogeneity of variance was tested using Levene's test. Paired samples t-test and Wilcoxon signed-rank test were used to compare paired numerical data, depending on normality. Independent samples t-test and Mann-Whitney U test were used for independent groups, and ANOVA and Kruskal-Wallis test were used for comparing multiple groups. Bonferroni correction was applied for post-hoc comparisons. The level of significance was set at $\alpha = 0.05$.

Results

Analysis of the flexural strength parameter, as presented in Table 2, revealed statistically significant differences among the groups according to the Kruskal-Wallis test. The STG (glazed) group demonstrated the highest flexural strength, followed by the STP (polished), NDG, NDP, FLP, PRG, HC, PRP, and FLG groups.

Concerning FS values, the HC group was superior to the PRP group, yet it was inferior to the FLP, NDP, and STP groups ($p < 0.05$).

While glazing enhanced the flexural strength of most 3D-printed groups, the FL group experienced a notable decrease ($p < 0.05$). The improvement in flexural strength for the ND group was not statistically significant ($p = 0.088$). Figure 2.

Microhardness analysis of the test specimens consistently revealed that, regardless of the surface treatment, the PR group exhibited the highest values across all groups, including HC ($p < 0.05$). In contrast, the ST group displayed the lowest, as shown in Fig. 3. and Table 2. Although glazing increased the microhardness of all 3D-printed groups ($p < 0.05$), this increase was not statistically significant for the ND group according to the Mann-Whitney U test ($p = 0.351$).

When the test samples were evaluated in terms of surface roughness, results indicated statistically significant differences between the mechanically polished (P) and glazed (G) groups before and after the coffee thermocycling procedure ($p < 0.05$). The comparative analysis of the influence of surface treatments and subsequent coffee thermocycling on the surface roughness (Ra) of various specimen groups is shown in Table 3.

Table 2 Results of the statistical analysis of Flexural strength (MPa), Vickers hardness and ΔE_{00}

Material	Surface treatment	ΔE_{00}		VH		FS	
		MD (Min-Max)	MN ± SD	MD (Min-Max)	MN ± SD	MD (Min-Max)	MN ± SD
Nextdent(ND)	Polishing(P)	3.09^{Ad} (2.4–3.45)	3.06 ± 0.23	18.75^{Ab} (17.33-20)	18.73 ± 0.7	110.04^{Ae} (92.51–126)	108.18 ± 8.51
	Glazing(G)	3.11^{Ad} (2.91–3.42)	3.12 ± 0.16	18.23^{Ab} (16.43–29.17)	18.9 ± 2.74	117.13^{Aef} (64.1-133.93)	111.29 ± 17.97
Powerresin(PR)	Polishing(P)	3.42^{Aef} (3.01–3.88)	3.4 ± 0.2	25.08^{Ad} (22.23–27.1)	24.72 ± 1.45	74.68^{Ab} (50.48–92.72)	73.72 ± 9.89
	Glazing(G)	3.35^{Ae} (2.92–3.64)	3.31 ± 0.22	26.17^{Be} (24.43–29.5)	26.53 ± 1.13	87.03^{Bcd} (73.25-103.33)	86.84 ± 8.95
Senertek(ST)	Polishing(P)	3.62^{Ag} (3.4–3.88)	3.61 ± 0.1	16.03^{Aa} (12.4-17.17)	15.96 ± 0.98	116.37^{Af} (102.17-136.18)	116.54 ± 10.26
	Glazing(G)	3.53^{Afg} (3.29–3.77)	3.53 ± 0.14	16.78^{Ba} (15-19.53)	16.88 ± 1.06	132.4^{Bg} (107.33-150.23)	132.87 ± 9.93
Formlabs(FL)	Polishing(P)	2.13^{Ac} (1.73–2.6)	2.1 ± 0.25	16.95^{Aa} (15.6-18.83)	17.1 ± 0.88	93.16^{Ad} (53.69-112.84)	90.76 ± 17.82
	Glazing(G)	1.86^{Bb} (1.31–2.47)	1.91 ± 0.31	23.67^{Bd} (16.77–32.23)	24.02 ± 4.16	41.89^{Ba} (22.88–53.15)	40.36 ± 8.58
Heat cured(HC)	Polishing(P)	1.4^{a} (0.9–1.78)	1.38 ± 0.23	20.25^{c} (18.83–22.53)	20.33 ± 0.85	82.05^{c} (74.6-85.44)	81.09 ± 3.29

* MN ± SD: Mean ± Standard Deviation, MD (Min-Max): Median (Minimum-Maximum)

** ΔE_{00}: Color change, VH: Vickers hardness, FS: Flexural strength

† Different uppercase letters indicate significant differences among polishing techniques within each material

‡ Different lowercase letters indicate significant differences among each materials and polishing techniques

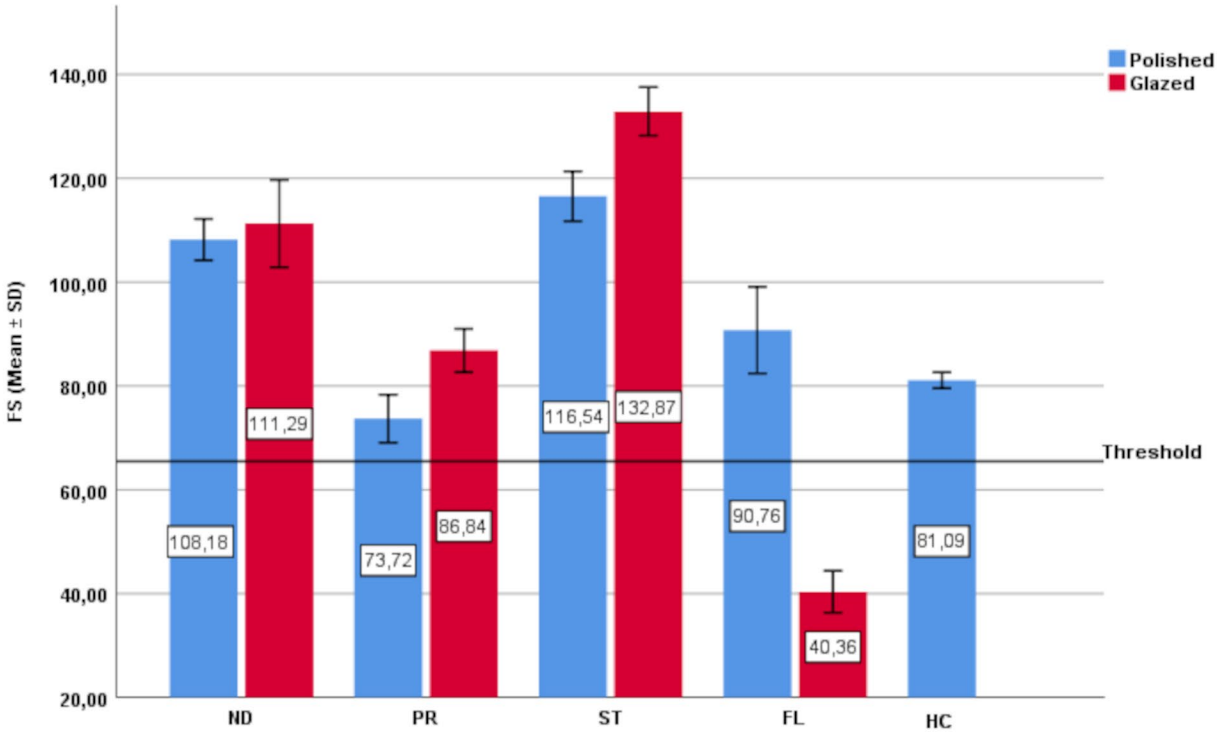

Fig. 2 Means of flexural strength values(MPa) according to the material and surface treatment

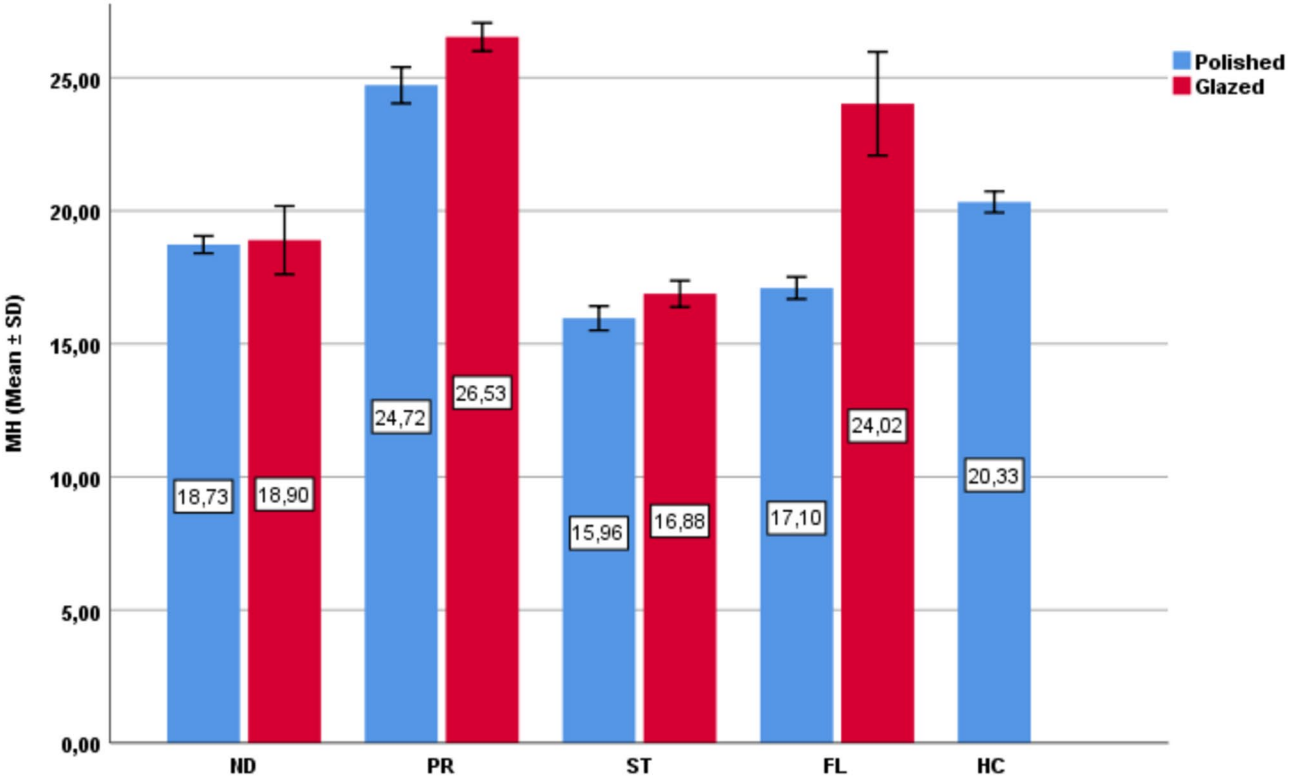

Fig. 3 Means of vickers microhardness values according to the material and surface treatment

Table 3 Results of the statistical analysis of roughness values (μm)

Material	Surface treatment	BCTC		ACTC	
		MD (Min-Max)	MN ± SD	MD (Min-Max)	MN ± SD
Nextdent (ND)	**Polishing (P)**	0.06^{dx} (0.03–0.07)	0.05 ± 0.01	0.12^{by} (0.1–0.36)	0.13 ± 0.05
	Glazing (G)	0.17^{Bx} (0.15–0.19)	0.17 ± 0.01	0.18^{Cy} (0.16–0.21)	0.18 ± 0.01
Powerresin (PR)	**Polishing (P)**	0.04^{cx} (0.03–0.05)	0.04 ± 0	0.13^{by} (0.11–0.14)	0.13 ± 0.01
	Glazing (G)	0.16^{Bx} (0.14–0.18)	0.16 ± 0.01	0.17^{By} (0.13–0.19)	0.17 ± 0.01
Senertek (ST)	**Polishing (P)**	0.02^{bx} (0.02–0.03)	0.02 ± 0	0.14^{by} (0.12–0.15)	0.14 ± 0.01
	Glazing (G)	0.18^{Cx} (0.15–0.21)	0.18 ± 0.01	**0.24^{Dy}(0.16–0.25)**	0.23 ± 0.02
Formlabs (FL)	**Polishing (P)**	0.01^{ax} (0.01–0.02	0.01 ± 0	0.1^{ay} (0.08–0.13)	0.1 ± 0.02
	Glazing (G)	0.13^{Ax} (0.12–0.14)	0.13 ± 0.01	0.15^{Ay} (0.13–0.16)	0.15 ± 0.01
Heat cured (HC)	**Polishing (P)**	0.04^{cx} (0.03–0.06)	0.04 ± 0.01	0.1^{ay} (0.06–0.12)	0.09 ± 0.02

* MN ± SD: Mean ± Standard Deviation, MD (Min-Max): Median (Minimum-Maximum)

**BCTC: Before coffee thermocycling, ACTC: After coffee thermocycling

† The uppercase letters represent the differences based on the glazed surface treatment, while the lowercase letters represent the differences based on the polished surface treatment

‡ x, y indicate significant differences among different time intervals within each material-polishing pair

Ra measurements on polished samples consistently revealed lower values than the glazed ones ($p < 0.05$) before and after coffee thermocycling. However, the mean difference in Ra values of the polished samples was bigger than that of the glazed ones after the thermocycling procedure. Among the mechanically polished groups, the NDP group exhibited the greatest Ra value (0.05 ± 0.01) before aging, followed by PRP, HC, STP, and FLP. After aging, the STP group demonstrated the highest Ra value (0.14 ± 0.01), with NDP, PRP, FLP, and HC following in descending order. The STG group exhibited the highest surface roughness within the glazed groups before and after thermal cycling (0.18 ± 0.01 and 0.23 ± 0.02, respectively), followed by NDG, PRG, and FLG.

Notably, except for the post-aging STG group's Ra value, all groups exhibited surface roughness values below the critical 0.2 μm threshold associated with plaque retention and microbial adhesion before and after coffee thermocycling. (Table 3)

ANOVA testing (Fig. 4.) showed that ΔE_{oo} significantly differed among all groups. The mean ΔE_{oo} in the conventional heat-cured (HC) group was significantly lower than that in the 3D-printed groups (1.38 ± 0.23). While glazing led to a reduction in ΔE_{oo} values, this effect was notably pronounced and statistically significant only within the Formlabs group ($p < 0.05$).

Regardless of the surface treatment, the ST group exhibited the highest ΔE_{oo} values among all 3D-printed groups, followed by PR, ND, and FL, respectively ($p < 0.05$). Furthermore, related to the clinical significance of color difference, according to the National Bureau of Standards (NBS) classification, the HC group exhibited a slight color change. The NDP, NDG, FLG, and FLP groups demonstrated a noticeable color change, whereas the STG, PRG, STP, and PRP groups showed an appreciable color change. (Fig. 5.)(Table 2).

SEM analysis revealed divergent fracture patterns between conventional and 3D-printed specimens. Conventional samples showed predominantly brittle fractures, while 3D-printed samples exhibited more intermediate fractures. Additionally, Vita Akzent glaze application on 3D-printed specimens significantly increased brittle fracture incidence. Figure 6.

Discussion

This study evaluated the flexural strength, microhardness, surface roughness, and color stability of one heat-cured and four 3D-printed resins, which underwent two surface treatments. The null hypothesis, which stated that there were no significant differences in flexural strength, microhardness, surface roughness, and color stability among conventional heat-polymerized PMMA and 3D-printed denture base resins with two distinct surface treatments after coffee thermocycling, was partially rejected.

Thermal cycling provides a valuable invitro methodology for simulating the intraoral environment and assessing the mechanical behavior of denture base materials. This cyclic temperature exposure induces water sorption within the denture base resins, leading to the degradation of the polymeric chains and a subsequent decline in mechanical properties. Furthermore, the absorbed water can hydrolyze the silane coupling agent, compromising the interfacial bond between the resin matrix and reinforcing fillers [6, 8, 31–33].

To simulate clinical service conditions, specimens were subjected to 5000 thermal cycles. While some studies have suggested that this cycle number may correspond to approximately six months of clinical service [14, 15, 34], other investigations have proposed that it may represent up to five years of clinical use [22, 31], highlighting the variability in the correlation between in vitro and in vivo conditions.

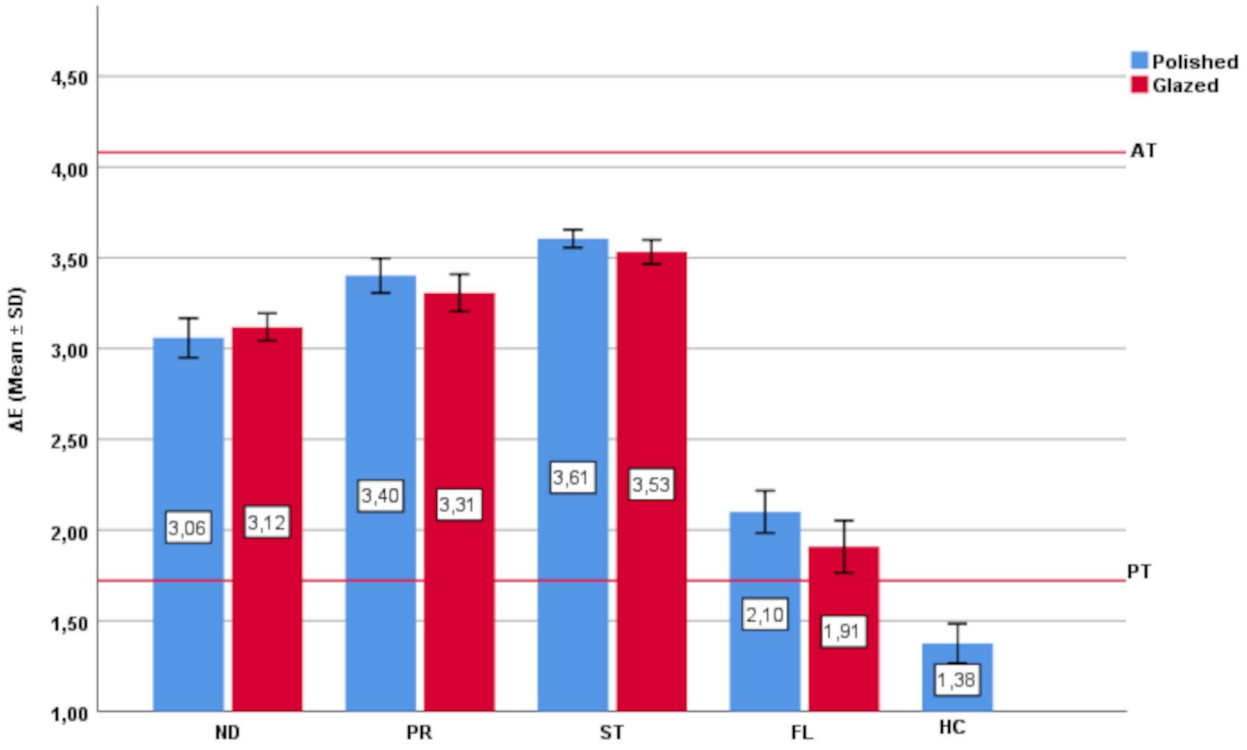

Fig. 4 Mean ΔE values after coffee thermal cycling
PT-perceptibility threshold(ΔE = 1,72); AT-acceptability threshold(ΔE = 4,08)

Microhardness (VH) reflects a material's resistance to localized plastic deformation when subjected to localized loads, such as those encountered during mastication of hard foods. Dentures with low microhardness are susceptible to surface damage from mechanical brushing, potentially resulting in pigmentation, plaque accumulation, and reduced service life [9, 20, 35–37]. The HC group exhibited significantly higher VH values regardless of surface treatment than the ST and ND 3D-printed groups. This observation aligns with previous research findings [15, 36], suggesting that lower residual monomer levels contribute to improved mechanical properties. It is well established that the uniform heating of PMMA during conventional fabrication methods results in greater monomer conversion, reduced plasticizing effects of residual monomers, and increased hardness [36]. Furthermore, the inherent structural differences between printed resins and those produced by heat-polymerization or CAD-CAM milling can influence their mechanical performance. Specifically, printed resins often exhibit lower double-bond conversion rates, potentially impacting their overall mechanical integrity [20]. Interestingly, the PR-printed group demonstrated even higher VH values than the HC and 3D-printed groups. This can be attributed to its post-curing under nitrogen atmosphere [10] and the high content of inorganic titanium dioxide filler (5–10%) [18, 20, 38].

The lower VH values observed in the ST group, characterized by a high UDMA content, can be attributed to the inherent flexibility of the UDMA ester bond, highlighting the significant influence of chemical composition on VH [36]. Glaze treatment resulted in a significant increase in microhardness.

(VH) values across all 3D-printed groups, except the ND group, where the increase was not statistically significant ($p > 0.05$). This finding aligns with previous research [20–22, 39] and can be attributed to incorporating silicon dioxide (SiO2) nanoparticles within the VitaAkzent glaze material [18, 20, 22, 39]. This enhancement in hardness can also be ascribed to a significant reduction in defects, such as scratches, which compromise surface hardness [20].

These evaluations made in the context of microhardness reflect the results of this study and compare the relevant test samples with each other. Since the threshold microhardness values required for total denture base resins are not defined in any standard [2], these data could not be evaluated in terms of clinical use.

Elevated flexural strength is paramount in preventing catastrophic failure of dentures subjected to masticatory forces. The three-point bending test utilized in this

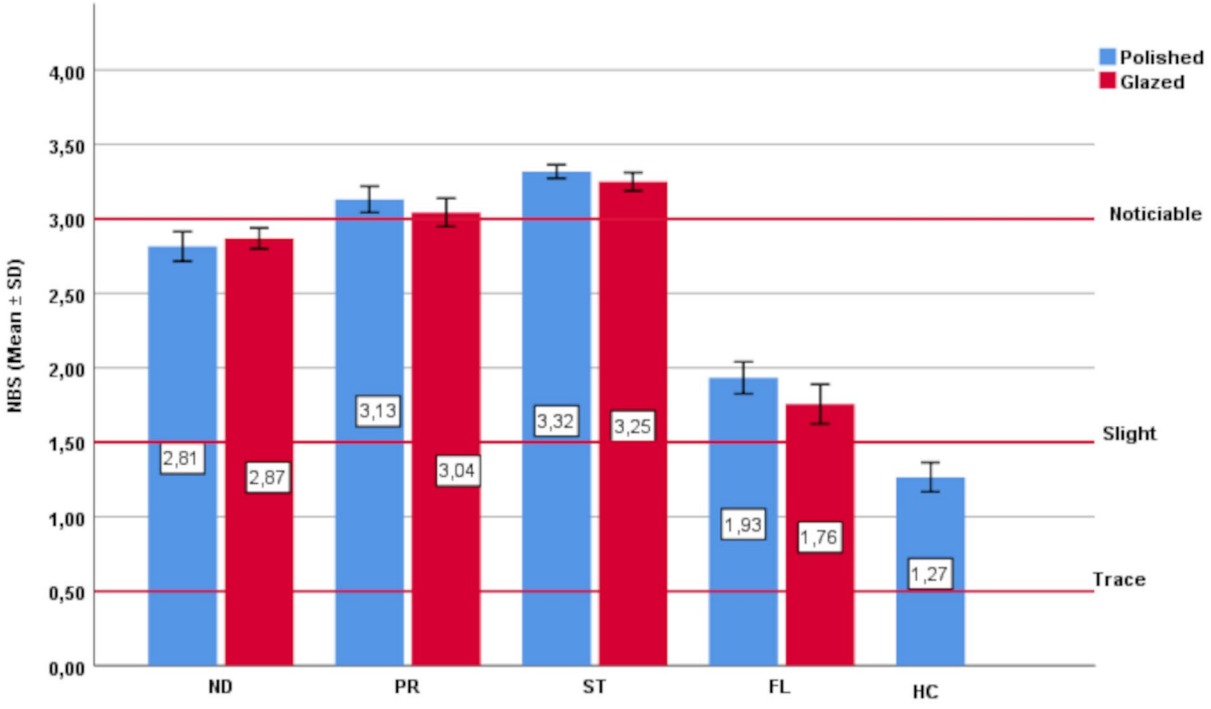

Fig. 5 Critical marks of color differences according to the National Bureau of standards(NBS). NBS classification: Trace (0.0–0.5); Slight (0.5–1.5); Noticeable (1.5–3.0); Appreciable (3.0–6.0)

investigation effectively replicates the loading conditions encountered by dentures during mastication [6, 9, 20].

Independent of surface treatment, the 3D-printed groups exhibited flexural strengths comparable to, or even exceeding, those of the HC group, aligning with some previous findings [4, 5, 8, 13, 33, 40]. This observation, however, contradicts the findings of Falahchai et al. and Prpić et al., who reported lower flexural strengths for 3D-printed groups compared to the HC group. This discrepancy can be attributed to those studies' significantly shorter post-curing times [15, 35].

Variations in material flexural strength can be attributed to several factors, including the polymerization process and the chemical composition of the resin [33, 36]. The superior flexural strength observed in the ST group can be attributed to the lower molar volume and molecular weight of the UDMA monomer. These characteristics likely contribute to an increased methacrylate functionality in the unpolymerized resin. This higher functionality facilitates a denser cross-linking network within the polymer matrix, ultimately enhancing flexural strength [13].

In the realm of 3D-printed denture base materials, printing orientation is a well-established factor influencing both flexural strength and accuracy [41–45]. While prior research has predominantly investigated the impact of standard orientations such as 0°, 45°, and 90°, findings regarding the optimal orientation remain inconsistent [41–42, 44, 46]. For instance, a systematic review by Alqutaibi et al., encompassing 24 studies on 3D-printed denture base resins, reported that the 0° orientation yielded the highest flexural strength values, with tilted and vertical orientations (90°) demonstrating a reduction [44]. Conversely, a recent study by Jafarpour et al. has indicated that a 90° printing orientation resulted in the highest flexural strength values [46]. These contradictory outcomes underscore the necessity for material-specific investigations, as the influence of printing orientation appears to be material-dependent [46]. In a comparative study of 120° and 130° printing orientations, Alharethi found no statistically significant difference in flexural strength between these angles [45]. In this study, oblique orientation (20°, 40°, and 60°) was implemented exclusively, adhering to the manufacturer's instructions. To the authors' knowledge, the current literature lacks specific research examining the effect of the 20°, 40°, and 60° printing orientations employed in this study. Consequently, a comprehensive discussion of the impact of these specific orientations based on existing literature is presently limited. Nevertheless, further investigation is warranted to validate assumptions and comprehensively

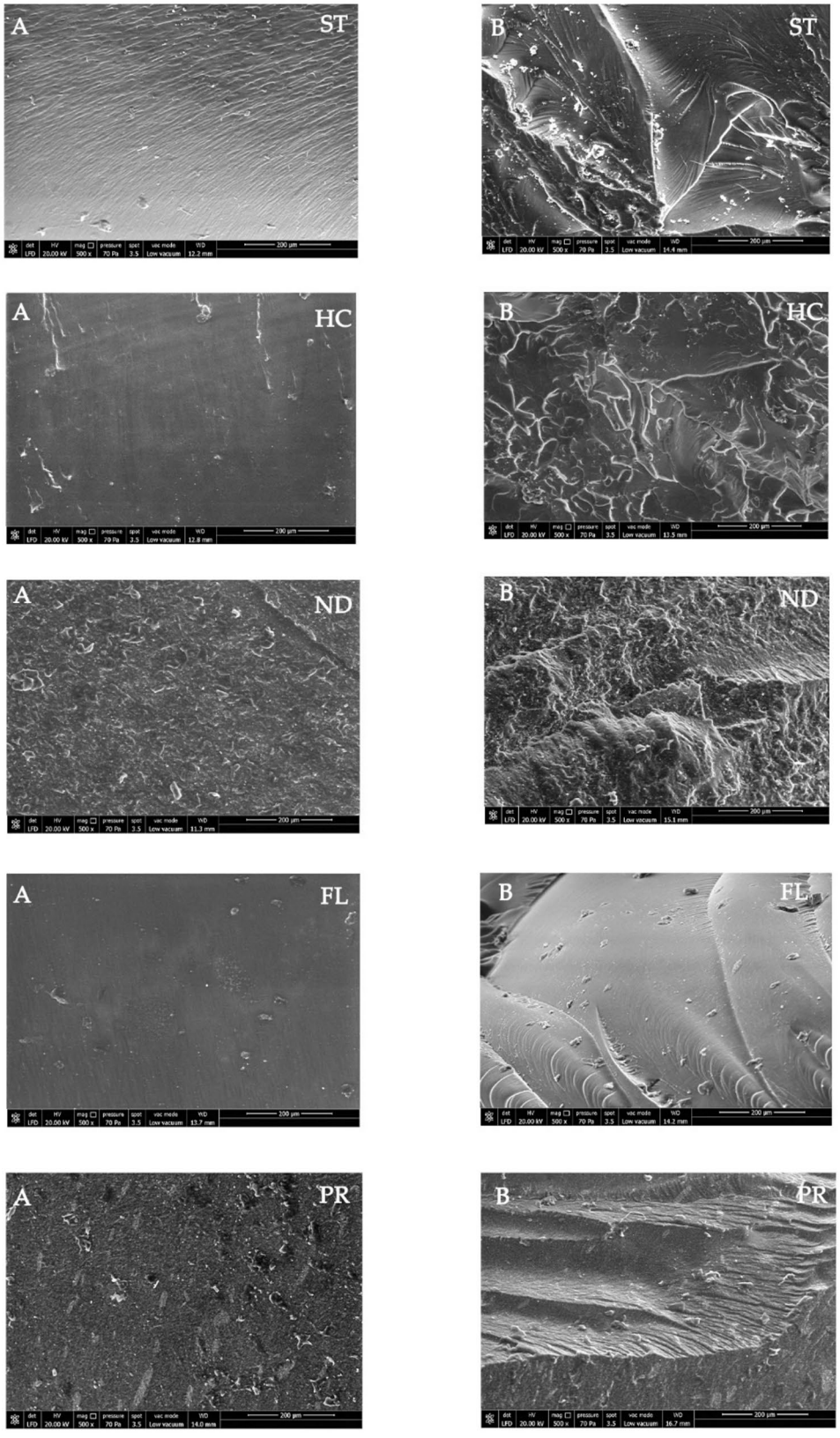

Fig. 6 SEM micrographs at 500x magnification reveal the fracture morphology of the specimens. (**A**) Smooth and compact fracture surfaces are indicative of a brittle fracture mode. (**B**) Jagged and rough fracture surfaces suggest an intermediate fracture mode
ST-Senertek; HC-heat cured; ND-Nextdent; PR-Powerresin; FL-Formlabs

elucidate the impact of alternative printing orientations beyond the conventional 0°, 45°, and 90°, on both the flexural strength of 3D-printed denture base materials.

Following glaze application, the ST and PR groups exhibited a statistically significant increase in flexural strength (FS), a result consistent with previous studies [22, 47]. This enhancement is attributable to the reinforcing effect of SiO2 nanoparticles as a filler, which facilitates interfacial cross-linking with the polymer matrix [18, 22, 47]. Azpiazu-Flores et al. reported a positive impact of Optiglaze material on the flexural strength (FS) and microhardness (VH) of 3D-printed denture base materials, noting that glazed specimens demonstrated higher FS values and sustained VH after thermocycling [22]. Conversely, the FL group experienced a decrease in FS after glaze application, a finding that, while contrary to some prior research [22, 47], aligns with the results of Carneiro Pereira et al. They postulated two potential mechanisms for this reduction: firstly, the formation of a rigid surface layer by the glaze, which may act as a brittle coating, diminishing the material's bending capacity and leading to stress concentrations and premature failure. Secondly, the presence of pendant methacrylate groups within the glaze composition, which may act as internal plasticizers at low strain rates, disrupting intermolecular forces and reducing flexural strength [20].

These conflicting results suggest that the effects of glaze application may vary depending on both the material and the specific glaze used. Consequently, further in-depth studies employing diverse glaze materials are warranted to elucidate these discrepancies. It is also crucial to acknowledge that while sandblasting enhances mechanical retention and adhesion of the glaze, it may negatively impact FS, potentially confounding results. Kang et al. found that sandblasting 3D-printed permanent restorations resulted in surface defects and cracks, leading to a deterioration of physical properties and decreased flexural strength [48].

The flexural strength values for conventional and 3D-printed groups, excluding the FLG group, exceeded the minimum acceptable value of 65 MPa for acrylic resins [25, 31, 35].

Previous studies have employed coffee solutions to assess changes in the surface roughness of acrylic resins, recognizing that coffee can decrease the pH of the oral environment and increase the solubility of acrylic resins [7, 15, 16].

Successful rehabilitation of edentulous patients necessitates prosthetic appliances that fulfill specific qualitative criteria, including a smooth resin surface. Various strategies are employed to mitigate microbial adhesion to denture surfaces, including mechanical or chemical polishing and surface coating techniques. Surfaces with high surface energy and roughness, particularly those with hydrophobic properties, may exhibit increased susceptibility to plaque accumulation. Ideally, denture base materials should not exceed a threshold of 0.2 µm. Rough surfaces promote microbial adhesion, plaque accumulation, halitosis, discoloration, and patient discomfort [2, 16, 18, 20, 49].

This study observed a significant increase in surface roughness (Ra) across all 3D-printed groups following glaze application, consistent with previous findings [17, 18, 23, 49]. This phenomenon, likely attributed to surface treatments such as sandblasting (often employed to improve glaze adhesion), can introduce surface irregularities, leading to uneven glaze distribution and subsequent fluctuations in surface smoothness [50, 51]. However, these findings contradict those of Alouthah et al., who reported a decrease in surface roughness of glazed denture bases, potentially due to using different glazing materials and the absence of sandblasting in their study [21].

Consistent with our findings, Bozogulları et al. observed a significant increase in surface roughness following glaze application. This aligns with the established understanding that glaze agents, particularly those with high viscosity and filler content, can impede homogenous spreading and contribute to surface irregularities [39].

Although the glaze application mitigated the impact of coffee thermocycling on Ra values, a statistically significant increase in Ra was still observed between pre-and post-treatment measurements. This may be attributed to the fact that VitaAkzent® (VA) glazes are chemically bonded sealants. While coffee thermocycling does not involve direct physical contact with the specimen surface, it may induce subtle changes within the coating. The cyclic temperature variations during this procedure could potentially lead to the formation of microcracks or the dislodgement of loosely adhered surface particles [17, 39].

Choi et al. reported the Ra values from 0.26 ± 0.01 to 0.15 ± 0.02 µm, which means that some denture coating materials exceed the threshold of 0.2 µm and may compromise the clinical performance of a complete denture they are applied [18]. In a Kraemer Fernandez et al. study, a single layer of the same unpolymerized denture resin material demonstrated a statistically greater Ra value of 0.16 ± 0.04 µm compared to the polished surface while remaining within the acceptable limit of 0.2 µm [23].

The lower Ra values observed in the HC group after CTC, regardless of surface treatment, can be attributed to several factors. 3D-printed resins often possess lower filler content, which, while advantageous for printability, may compromise wear resistance and surface durability. Settling fillers during storage can further exacerbate this issue, leading to inhomogeneous layers and impaired polymerization [29, 37].

In this study, coffee thermocycling increased all Ra values regardless of the surface treatment. This result is consistent with the findings of previous studies [15, 16, 26]. However, it contradicts the results of some studies. Çakmak et al. [2] found that coffee thermocycling did not affect Ra values. These discrepancies highlight the need for further research and longer thermal cycles [2].

Coffee has been reported to change the color of 3D-printed resin specimens significantly. The increased susceptibility to discoloration observed in 3D-printed groups may be attributed to a confluence of factors, including elevated Ra values following CTC, inherent chemical heterogeneity, and potentially lower conversion degrees than HC resin [15, 16, 29].

The HC group exhibited the least color change following thermocycling, a finding consistent with previous studies [15, 29]. Higher water sorption after thermocycling in the 3D-printed resins than in the conventional heat-polymerizing resin has been reported to degrade dental resins and enhance the attachment of pigments [3, 28, 37, 52]. Conversely, the findings of Alfouzan et al. [14] diverge from this present investigation, revealing superior color stability in 3D-printed denture base materials compared to conventional counterparts. This discrepancy may be attributed to variations in the materials evaluated and the experimental methodologies employed in the respective study.

All specimen groups were fabricated using an identical layer thickness of 50 µm, in accordance with the manufacturers' specifications. While Çakmak et al. reported no significant effect of layer thickness (50 µm vs. 100 µm) on the stainability of 3D-printed denture base resins [2], Lee et al. demonstrated a notable influence of layer thickness on the color stability of these materials. Therefore, maintaining a consistent layer thickness of 50 µm across all groups in the present study was deemed crucial to minimize variability and ensure the reliability of the comparative color stability analysis [7].

Although glazing decreased color change in all groups, the reduction was statistically significant solely for the Formlabs group. The glaze application resulted in a marked reduced ΔE_{00} value, specifically for Formlabs materials. This finding aligns with the glaze's ability to diminish water absorption [53], a known factor in material degradation and discoloration. Nonetheless, empirical evidence from future research is required to substantiate this claim. A glazed surface layer acts as a barrier, mitigating the penetration of colored pigments and consequently reducing ΔE_{00} values compared to unglazed surfaces [47].

Nam et al. [47] reported a decrease in ΔE value with the use of glaze materials, attributing this to the fact that glazed resin restorations consist of a light-curing transparent resin coating that permeates the resin surface, filling micropores and defects, and consequently reducing porosity and microleakage [47, 54].

Regardless of the surface treatment, color changes exceeded the perceptible threshold ($\Delta E_{00} = 1.72$) for all three printed groups. However, none of the color deviations exceeded the acceptable threshold ($\Delta E_{00} = 4.08$), indicating no unacceptable color shift [27].

Scanning electron microscopy (SEM) micrographs revealed a predominance of brittle fracture modes in the conventional group, whereas the 3D-printed group exhibited a significantly higher frequency of intermediate fracture modes. This observation is consistent with findings reported in prior studies and can be attributed to the enhanced impact strength and increased flexibility of the 3D-printed specimens compared to their conventional counterparts [15, 30].

The elevated incidence of brittle fractures detected in Vita Akzent-coated specimens, as substantiated by scanning electron microscopy (SEM) imaging, aligns with observations documented in a previous investigation [22]. This phenomenon is attributable to the reinforcing effect of the homogeneous Vita Akzent layer, which promotes stress distribution across an expanded surface area of the specimen [22]. Consequently, this stress dispersion mechanism is hypothesized to contribute to an augmentation in flexural strength, a conclusion consistent with our empirical findings. Specifically, the PRG and STG groups demonstrated a statistically significant enhancement in flexural strength, thereby validating this interpretation. Conversely, the FLG group did not exhibit a increase in flexural strength. This observed disparity in fracture patterns underscores the critical need for a quantitative analytical approach, rather than a solely qualitative assessment, to comprehensively elucidate the influence of the glaze material on fracture behavior.

Limitations and future scope

This study presents several limitations that warrant consideration. Firstly, the lack of mechanical aging protocols may have limited the assessment of long-term material degradation. Secondly, the use of a single glaze brand may restrict a comprehensive under-standing of glaze effects. Furthermore, crucial aspects such as water sorption, solubility, surface wettability, and biofilm adherence were not investigated. The influence of sandblasting, polymerization, and glaze flaking also require further investigation. Future studies should focus on developing protocols for glaze maintenance and reapplication, establish standardized glazing protocols for CAD-CAM denture base materials, and explore the effects of various glaze compositions and application methods under oral conditions.

Conclusions

The polishing technique and the subsequent coffee thermocycling influenced the surface roughness of the tested materials. Conventional polishing yielded smoother surfaces compared to glazed surfaces. Except for the ST group treated with Vita Akzent, all roughness values remained below the acceptable threshold of 0.2 µm.

Material type significantly influenced the stainability of the tested materials. While glazing effectively reduced color change in Formlabs materials, this effect was not statistically significant for other materials. Nevertheless, the magnitude of color change observed between polishing pairs remained within acceptable limits for all tested materials.

Incorporating Vita Akzent glaze material into 3D-printed denture bases enhanced hardness and improved wear resistance. However, the effect of Vita Akzent on flexural strength varied significantly across different materials. While it positively impacted the flexural strength of the ST and PR groups, it led to a substantial decrease in flexural strength within the FL group. The effect on the ND group was negligible.

Developing a standardized polishing protocol specifically for 3D-printed denture base materials is crucial. Furthermore, this study's findings demonstrate the superior effectiveness of mechanical polishing in reducing surface roughness compared to glazing techniques.

Abbreviations

CAD-CAM	Computer-aided design and computer-aided manufacturing
ND	NextDent
FL	FormLabs
ST	Senertek
PR	Powerresin
HC	Heat cured
G	Glazed
P	Polished
3D	3-dimensional
CDs	Complete dentures
STL	Standard tessellation language
ISO	International Organization for Standardization
PT	Perceptibility threshold
AT	Acceptability threshold

Acknowledgements

Not applicable.

Author contributions

Eİ and EE made equal contributions to the conceptualization, methodology, validation, formal analysis, investigation, resources, data curation, writing-review & editing, and visualization. EE was responsible for the supervision and project administration. All authors have read and approved the final manuscript.

Funding

This research received no external funding. No financial support was received for this project.

Data availability

The datasets used and/or analysed during the current study are available from the corresponding author on reasonable request.

Declarations

Ethics approval and consent to participate

Not applicable.

Consent for publication

Not applicable.

Competing interests

The authors declare no competing interests.

Author details

[1]Department of Prosthodontics, Faculty of Dentistry, Suleyman Demirel University, Isparta 32000, Turkey

Received: 1 February 2025 / Accepted: 24 April 2025
Published online: 30 April 2025

References

1. Kattadiyil MT, Al Helal A, Goodacre BJ. Clinical complications and quality assessments with computer-engineered complete dentures: A systematic review. J Prosthet Dent. 2017;117(6):721–8.
2. Çakmak G, Asadolahi NW, Schimmel M, Molinero-Mourelle P, Akay C, Donmez MB, et al. Effect of coffee thermal cycling on the surface properties and stainability of additively manufactured denture base resins in different layer thicknesses. J Prosthodont. 2023 Nov;15:1–10. https://doi.org/10.1111/jopr.13803.
3. Gad MM, Alshehri SZ, Alhamid SA, Albarrak A, Khan SQ, Alshahrani FA, et al. Water sorption, solubility, and translucency of 3D-Printed denture base resins. Dent J. 2022;10(3):42.
4. Li R, Malik D, Sadid-Zadeh R. Effect of adding a hard-reline material on the flexural strength of conventional, 3D-printed, and milled denture base materials. J Prosthet Dent. 2023;129(5):e7961–7.
5. Fiore AD, Meneghello R, Brun P, Rosso S, Gattazzo A, Stellini E, et al. Comparison of the flexural and surface properties of milled, 3D-printed, and heat polymerized PMMA resins for denture bases: an in vitro study. J Prosthodont Res. 2022;66(3):502–8.
6. Samahy E MM, A AM, Shabrawy E SM, H KI. Evaluation of physicomechanical properties of milled versus 3D-printed denture base resins: A comparative in vitro study. J Prosthet Dent. 2023;129(5):e7971–7.
7. Lee EH, Ahn JS, Lim YJ, Kwon HB, Kim MJ. Effect of layer thickness and printing orientation on the color stability and stainability of a 3D-printed resin material. J Prosthet Dent. 2022;127(5):e7841–7.
8. Li R, Albaghli A, Orgev A, Marrano J, Sadid-Zadeh R. Effect of thermal cycling on the flexure strength of CAD-CAM denture base materials: an in vitro study. J Prosthet Dent. 2024;132(3):e6451–7.
9. Vuksic J, Pilipovic A, Poklepovic Pericic T, Kranjcic J. The influence of contemporary denture base fabrication methods on residual monomer content, flexural strength and microhardness. Materials. 2024;17(5):1052.
10. Lee WJ, Jo YH, Yoon HI. Influence of postpolymerization time and atmosphere on the mechanical properties, degree of conversion, and cytotoxicity of denture bases produced by digital light processing. J Prosthet Dent. 2023;130(2):e2651–7.
11. Caussin E, Moussally C, Le Goff S, Fasham T, Troizier-Cheyne M, Tapie L, et al. Vat photopolymerization 3D printing in dentistry: A comprehensive review of actual popular technologies. Materials. 2024;17(4):950.
12. Piedra-Cascón W, Krishnamurthy VR, Att W, Revilla-León M. 3D printing parameters, supporting structures, slicing, and post-processing procedures of vat-polymerization additive manufacturing technologies: A narrative review. J Dent. 2021;109:103630.
13. Casucci A, Verniani G, Barbieri AL, Ricci NM, Ferrari Cagidiaco E, Ferrari M. Flexural strength analysis of different complete denture Resin-Based materials obtained by conventional and digital manufacturing. Materials. 2023;16(19):6559.
14. Alfouzan AF, Alotiabi HM, Labban N, Al-Otaibi HN, Al Taweel SM, AlShehri HA. Color stability of 3D-printed denture resins: effect of aging, mechanical brushing and immersion in staining medium. J Adv Prosthodont. 2021;13(3):160.
15. Falahchai M, Ghavami-Lahiji M, Rasaie V, Amin M, Neshandar Asli H. Comparison of mechanical properties, surface roughness, and color stability of

3D-printed and conventional heat-polymerizing denture base materials. J Prosthet Dent. 2023;130(2):266.e1-266.e8.
16. Çakmak G, Weber FA, Donmez MB, Kahveci Ç, Schimmel M, Yilmaz B. Effect of coffee thermocycling on the surface roughness and stainability of denture base materials with different chemical compositions manufactured with additive and subtractive technologies. J Esthet Restor Dent. 2024;36(3):453–9.
17. Çakmak G, Oosterveen-Rüegsegger AL, Akay C, Schimmel M, Yilmaz B, Donmez MB. Influence of Polishing technique and coffee thermal cycling on the surface roughness and color stability of additively and subtractively manufactured resins used for definitive restorations. J Prosthodont. 2024;33(5):467–74.
18. Choi JJE, Uy CE, Ramani RS, Waddell JN. Evaluation of surface roughness, hardness and elastic modulus of nanoparticle containing light-polymerized denture glaze materials. J Mech Behav Biomed Mater. 2020;103:103601.
19. Sulaya K, V SB, Nayak VM. The science of printing and Polishing 3D-printed dentures. F1000Res. 2025;13:1266. https://doi.org/10.12688/f1000research.157596.2.
20. Carneiro Pereira AL, Dos Santos Silva JP, Grangeiro MTV, de Medeiros AKB, Bottino MA, Barão VAR, et al. 3D-printed denture base resins: glazing as an alternative to improve surface, mechanical, and Microbiological properties. J Prosthodont. 2024;1–12. https://doi.org/10.1111/jopr.14001.
21. Alouthah H, Lippert F, Yang C, Levon JA, Lin W. Comparison of surface characteristics of denture base resin materials with two surface treatment protocols and simulated brushing. J Prosthodont. 2023;jopr.13794.
22. Azpiazu-Flores FX, Elfana A, Yang CC, Morton D, Lin WS. Effect of artificial aging and different surface finishing protocols on the flexural strength and surface hardness of a photopolymer for manufacturing monolithic polychromatic complete dentures using polyjet 3D printing. J Prosthodont. 2024;1–9. https://doi.org/10.1111/jopr.13963.
23. Kraemer Fernandez P, Unkovskiy A, Benkendorff V, Klink A, Spintzyk S. Surface characteristics of milled and 3D printed denture base materials following Polishing and coating: an In-Vitro study. Materials. 2020;13(15):3305.
24. Cohen J. Statistical power analysis for the behavioral sciences. 2nd ed. Hoboken: Taylor and Francis; 2013. P.273–403.
25. International Organization for Standardization (ISO). ISO 20795-1:2013 [Internet]. Geneva, Switzerland. 2013. Available from: https://www.iso.org/standard/62277.html
26. Alp G, Johnston WM, Yilmaz B. Optical properties and surface roughness of prepolymerized poly(methyl methacrylate) denture base materials. J Prosthet Dent. 2019;121(2):347–52.
27. Ren J, Lin H, Huang Q, Zheng G. Determining color difference thresholds in denture base acrylic resin. J Prosthet Dent. 2015;114(5):702–8.
28. Gad MA, Abdelhamid AM, ElSamahy M, Abolgheit S, Hanno KI. Effect of aging on dimensional accuracy and color stability of CAD-CAM milled and 3D-printed denture base resins: a comparative in-vitro study. BMC Oral Health. 2024;24(1):1124.
29. Gruber S, Kamnoedboon P, Özcan M, Srinivasan M. CAD/CAM complete denture resins: an in vitro evaluation of color stability. J Prosthodont. 2021;30(5):430–9.
30. Al-Dwairi ZN, Al Haj Ebrahim AA, Baba NZ. A comparison of the surface and mechanical properties of 3D printable Denture-Base resin material and conventional polymethylmethacrylate (PMMA). J Prosthodont. 2023;32(1):40–8.
31. Viotto HEDC, Silva MDD, Nunes TSBS, Coelho SRG, Pero AC. Effect of repair methods and materials on the flexural strength of 3D-printed denture base resin. J Adv Prosthodont. 2022;14(5):305.
32. Çakmak G, Donmez MB, Akay C, Abou-Ayash S, Schimmel M, Yilmaz B. Effect of thermal cycling on the flexural strength and hardness of New-Generation denture base materials. J Prosthodont. 2023;32(S1):81–6.
33. Temizci T, Bozoğulları HN. Effect of thermal cycling on the flexural strength of 3-D printed, CAD/CAM milled and heat-polymerized denture base materials. BMC Oral Health. 2024;24(1):357.
34. Gale MS, Darvell BW. Thermal cycling procedures for laboratory testing of dental restorations. J Dent. 1999;27(2):89–99.
35. Prpić V, Schauperl Z, Ćatić A, Dulčić N, Čimić S. Comparison of mechanical properties of 3D-Printed, CAD/CAM, and conventional denture base materials. J Prosthodont. 2020;29(6):524–8.
36. Aati S, Akram Z, Shrestha B, Patel J, Shih B, Shearston K, et al. Effect of post-curing light exposure time on the Physico–mechanical properties and cytotoxicity of 3D-printed denture base material. Dent Mater. 2022;38(1):57–67.
37. Arora O, Ahmed N, Siurkel Y, Ronsivalle V, Cicciù M, Minervini G. A comparative evaluation of physical properties of CAD/CAM complete denture resins-an in vitro study. BMC Oral Health. 2024;24(1):65.
38. Mhaibes AH, Safi IN, Haider J. The influence of the addition of titanium oxide nanotubes on the properties of 3D printed denture base materials. J Esthet Restor Dent. 2024;36(11):1574–90.
39. Bozoğulları HN, Büyükerkmen EB, Büyüközer Özkan H. Comparison of surface roughness and color stability of different denture characterizing composite resins: the effect of different surface treatments. J Prosthodont. 2023;32(S1):53–60.
40. Lawson NC, Safadi Y, Alford A, Aggarwal H, Bora PV, Lawson TJ et al. Flexural strength, fracture toughness, translucency, stain resistance, and water sorption of 3D-printed, milled, and conventional denture base materials. J Prosthodont.2024;1_8.https://doi.org/10.1111/jopr.13955
41. Altarazi A, Haider J, Alhotan A, Silikas N, Devlin H. Assessing the physical and mechanical properties of 3D printed acrylic material for denture base application. Dent Mater. 2022;38(12):1841–54.
42. Al-Dulaijan YA, Alsulaimi L, Alotaibi R, Alboainain A, Akhtar S, Khan SQ, et al. Effect of printing orientation and post curing time on the flexural strength of 3D-Printed resins. J Prosthodont. 2023;32(S1):45–52.
43. Song S, Zhang J, Liu M, Li F, Bai S. Effect of build orientation and layer thickness on manufacturing accuracy, printing time, and material consumption of 3D printed complete denture bases. J Dent. 2023;130:104435.
44. Alqutaibi AY, Aljohani R, Almuzaini S, Alghauli MA. Physical–mechanical properties and accuracy of additively manufactured resin denture bases: impact of printing orientation. J Prosthodont Res. 2025. https://doi.org/10.2186/jpr.JPR_D_24_00263.
45. Alharethi NA. Evaluation of the influence of build orientation on the surface roughness and flexural strength of 3D-Printed denture base resin and its comparison with CAD-CAM milled denture base resin. Eur J Dent. 2023;18:321–8.
46. Jafarpour D, El-Amier N, Tahboub K, Zimmermann E, Pero AC, de Souza R. Effects of DLP printing orientation and postprocessing regimes on the properties of 3D printed denture bases. J Prosthet Dent. 2025. https://doi.org/10.1016/j.prosdent.2025.02.035.
47. Nam NE, Hwangbo NK, Kim JE. Effects of surface glazing on the mechanical and biological properties of 3D printed permanent dental resin materials. J Prosthodont Res. 2024;68(2):273–82.
48. Kang YJ, Kim H, Lee J, Park Y, Kim JH. Effect of airborne particle abrasion treatment of two types of 3D-printing resin materials for permanent restoration materials on flexural strength. Dent Mater. 2023;39(7):648–58.
49. Yarar S, Değer Y, Tekin S. Effect of different Polishing methods applied to denture base materials on microbial adhesion and surface roughness. J Med Dent Investig. 2023;4:e230351–230351.
50. Sabbah A, Romanos G, Delgado-Ruiz R. Extended Post-Curing light exposure and sandblasting effects on surface hydrophobicity of 3D-Printed denture base resin. Prosthesis. 2022;4(1):80–90.
51. Kara D, Tekçe N, Fidan S, Demirci M, Tuncer S, Balcı S. The effects of various Polishing procedures on surface topography of CAD/CAM resin restoratives. J Prosthodont. 2021;30(6):481–9.
52. Greil V, Mayinger F, Reymus M, Stawarczyk B. Water sorption, water solubility, degree of conversion, elastic indentation modulus, edge chipping resistance and flexural strength of 3D-printed denture base resins. J Mech Behav Biomed Mater. 2023;137:105565.
53. Cakan U, Kara HB. Effect of liquid Polishing materials on the stainability of bis-acryl interim restorative material in vitro. J Prosthet Dent. 2015;113(5):475–9.
54. Sahin O, Koroglu A, Dede DÖ, Yilmaz B. Effect of surface sealant agents on the surface roughness and color stability of denture base materials. J Prosthet Dent. 2016;116(4):610–6.

Publisher's note